

A discussion on the anomalous threshold enhancement of $J/\psi - \psi(3770)$ couplings and $X(6900)$ peak

December 19, 2023

YE LU[†], CHANG CHEN^{††}, GUANG-YOU QIN[†], HAN-QING ZHENG[∞]

[†] *Institute of Particle Physics and Key Laboratory of Quark and Lepton Physics (MOE), Central China Normal University, Wuhan, Hubei 430079, China*

^{††} *Department of Physics, Peking University, Beijing 100871, China*

[∞] *College of Physics, Sichuan University, Chengdu, Sichuan 610065, China*

Abstract

The attractive interaction between J/ψ and $\psi(3770)$ has to be strong enough to form the molecular resonant structure, i.e., $X(6900)$. We argue that since $\psi(3770)$ decays predominantly into a $D\bar{D}$ pair, the interactions between J/ψ and $\psi(3770)$ may be significantly enhanced due to the three point $D\bar{D}$ loop diagram. The enhancement comes from the anomalous threshold located at $t = -1.288\text{GeV}^2$, which effect propagates into the s -channel partial wave amplitude in the vicinity of $\sqrt{s} \simeq 6.9\text{GeV}$. This effect may be helpful in forming the $X(6900)$ peak.

The $X(6900)$ peak observed by the LHCb Collaboration in the di- J/ψ invariant mass spectrum [1] [2], and later in the $J\psi\psi(3686)$ invariant mass spectrum [3]. has stimulated many discussions in theory aspects (see for example Ref. [4] for an incomplete list of references). On the other side, since $X(6900)$ is close to the threshold of $J/\psi\psi(3770)$, $J/\psi\psi_2(3823)$, $J/\psi\psi_3(3842)$, and $\chi_{c0}\chi_{c1}$ (and $X(7200)$ is close to the threshold of $J/\psi\psi(4160)$ and $\chi_{c0}\chi_{c1}(3872)$), inspired by this, it is studied in Ref. [5] the properties of $X(6900)$ and $X(7200)$, by assuming the $X(6900)$ coupling to $J/\psi J/\psi$, $J/\psi\psi(3770)$, $J/\psi\psi_2(3823)$, $J/\psi\psi_3(3842)$ and $\chi_{c0}\chi_{c1}$ channels, and $X(7200)$ to $J/\psi J/\psi$, $J/\psi\psi(4160)$ and $\chi_{c0}\chi_{c1}(3872)$ channels. For the S -wave $J/\psi J/\psi$ coupling, the pole counting rule (PCR) [6], which has been applied to the studies of “ XYZ ” physics in Refs. [7–10] is employed to analyze the nature of the two structures. It is found that the di- J/ψ data alone is not enough to judge the intrinsic properties of the two states. It is also pointed out that the $X(6900)$ is unlikely a molecule of $J/\psi\psi(3686)$ [5] – a conclusion drawn before the discovery of Ref. [3]. More recently, Refs. [4, 11, 12] made an analysis on $X(6900)$ using a combined analysis on di- J/ψ and $J/\psi\psi(3686)$ data and concluded that $X(6900)$ cannot be a $J/\psi\psi(3686)$ molecule.

Nevertheless, as already stressed in Ref. [4], even though $X(6900)$ is very unlikely a molecule of $J/\psi\psi(3686)$, it does not mean that it has to be an “elementary state” (i.e., a compact $\bar{c}ccc$ tetraquark state). It is pointed out that, it is possible that $X(6900)$ be a molecular state composed of other particles, such as $J/\psi\psi(3770)$, which form thresholds closer to $X(6900)$, if the channel coupling is sufficiently large.

This note will discuss a possible mechanism for the enhancement of the $J/\psi\psi(3770)$ channel coupling. The $D\bar{D}$ (or $D^*\bar{D}^*$) component inside $\psi(3770)$ may play an important role, so far ignored in the literature, in explaining the $X(6900)$ resonant peak, through the anomalous threshold emerged from the triangle diagram generated by D (D^*) loop, as depicted in Fig. 1.

Noticing that $\psi(3770)$ or ψ'' couples dominantly to $D\bar{D}$, we start from the Feynman diagram as depicted in Fig. 1 by assuming it contributes $J/\psi\psi''$ elastic scatterings near $J/\psi\psi''$ threshold.

¹ Assuming an interaction lagrangian²

¹It could be wondered that the $X(6900)$ be a $\bar{D}D J/\psi$ three body halo state, see Refs. [14, 15].

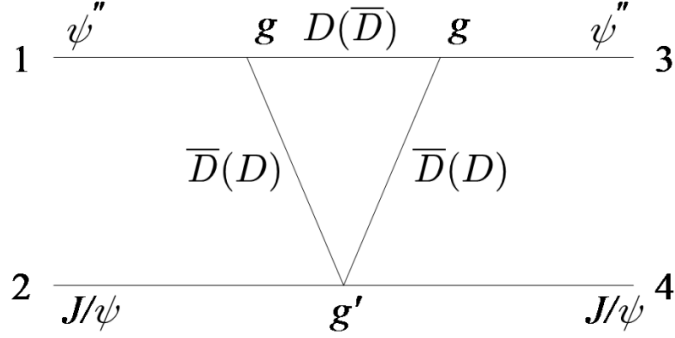


Figure 1: The $D\bar{D}$ triangle diagram in $J/\psi\psi''$ scattering process.

$$\mathcal{L} = -ig(D^0\partial_\mu\bar{D}^0 - \bar{D}^0\partial_\mu D^0)\psi''^\mu - ig(D^+\partial_\mu D^- - D^-\partial_\mu D^+)\psi''^\mu + g'D^0\bar{D}^0 J/\psi^\mu J/\psi_\mu + g'D^+D^- J/\psi^\mu J/\psi_\mu, \quad (1)$$

after performing the momentum integration the amplitude as depicted by Fig. 1 is

$$i\mathcal{M} = (-16g^2g') (\epsilon_2 \cdot \epsilon_4) \epsilon_1^\mu \epsilon_3^\nu \int d^D k \frac{k_\mu k_\nu}{((k-p_1)^2 - m_D^2)((k-p_3)^2 - m_D^2)(k^2 - m_D^2)} \quad (2)$$

$$\equiv (-16g^2g') (\epsilon_2 \cdot \epsilon_4) \epsilon_1^\mu \epsilon_3^\nu \mathcal{A}_{\mu\nu}$$

where

$$\mathcal{A}^{\mu\nu} = \frac{-i}{16\pi^2} \int_0^1 dx \int_0^{1-x} dy \left\{ \frac{p_3^\mu p_1^\nu xy}{\Delta} - \frac{g^{\mu\nu}}{4} \Gamma(\epsilon) \frac{1}{\Delta^\epsilon} \right\} \quad (3)$$

$$\equiv \frac{-i}{16\pi^2} \left\{ p_3^\mu p_1^\nu \mathcal{B} + \int_0^1 dx \int_0^{1-x} dy \left(-\frac{g^{\mu\nu}}{4} \Gamma(\epsilon) \frac{1}{\Delta^\epsilon} \right) \right\},$$

and

$$\mathcal{B}(t) = \int_0^1 dx \frac{x}{2M^2} \left(2(M^2(1-2x) + tx) \frac{\text{ArcTan}(\frac{M^2-tx}{\Lambda(t,x)}) - \text{ArcTan}(\frac{M^2(2x-1)-tx}{\Lambda(t,x)})}{\Lambda(t,x)} \right. \quad (4)$$

$$\left. + \ln \frac{m^2 + t(x-1)x}{m^2 + M^2(x-1)x} \right).$$

In above $\Lambda(t,x) = \sqrt{4m^2M^2 - M^4 + 4M^2tx^2 - 2M^2tx - t^2x^2}$, $\Delta = M^2(x^2 + y^2) + (2M^2 - t)xy - M^2(x+y) + m^2$, $\Gamma(\epsilon) \frac{1}{\Delta^\epsilon} = \frac{1}{\epsilon} - \ln \Delta - \gamma + \ln 4\pi + \mathcal{O}(\epsilon)$. On the right hand side of Eq. (3), only the \mathcal{B} term will be considered since the rest will be absorbed by the contact interactions to be introduced latter. M is the mass of $\psi(3770)$, m is the mass of $D(\bar{D})$. The parameter g is the coupling strength of $\psi'' D\bar{D}$ three point vertex, g' the coupling strength of $J/\psi J/\psi D\bar{D}$ four point vertex; $t = (p_2 - p_4)^2$. The parameter g can be determined by the process $\psi'' \rightarrow D^0\bar{D}^0$ decay,

$$i\mathcal{M}_{\psi'' DD} = ig\epsilon(\psi'') \cdot [p(D^0) - p(\bar{D}^0)], \quad (5)$$

$$\Gamma = \frac{1}{8\pi} |i\mathcal{M}_{\psi'' DD}|^2 \frac{q(DD)}{M_{\psi''}^2} = \frac{1}{6\pi} g^2 \frac{q(DD)^3}{M_{\psi''}^2},$$

where $q(DD)$ is the norm of three-dimensional momentum of D^0 or \bar{D}^0 in final state. The PDG value $\Gamma_{\psi'' \rightarrow D^0\bar{D}^0} \sim 27.2 \times 52\% \times 10^{-3}$ [16] determines $g \sim 12$.³ Parameter g' is unknown and left as a free parameter. The amplitude Eq. (4) contains rather complicated singularity structure, especially the well-known anomalous threshold, which in history was discovered by

²We neglect all the complexities such as form factors, hence our calculations are only qualitative or at best semi-quantitative.

³In Ref. [17], g is estimated to be larger (~ 30).

Mandelstam who use it to explain the looseness of deuteron wave function [13]. The anomalous threshold locates at

$$s_A = 4m^2 - \frac{(M^2 - 2m^2)^2}{m^2}. \quad (6)$$

Putting the mass of ψ'' and D^0 mesons, one gets $s_A = -1.28\text{GeV}^2$ (for D^+ loop, -0.98GeV^2). Numerically function \mathcal{B} is plotted in Fig. 2a, where one clearly sees the anomalous threshold, beside the normal one at $t = 4m^2$. Notice that if M^2 were smaller than $2m^2$, the anomalous branch point locates below physical threshold, but on the second sheet. It touches the physical threshold $4m^2$ and turns up to the physical sheet if the value of M^2 increased to $2m^2$. When further increase M^2 , the anomalous threshold moves towards left on the real axis and pass the origin when $M^2 = 4m^2$, and finally reach the physical value, i.e., -1.28GeV^2 . The situation is depicted in Fig. 2b. Notice that s_A here is negative, contrary to what happens in deuteron, because the latter is a bound state with a normalizable wave function, whereas ψ'' is an unstable resonance.

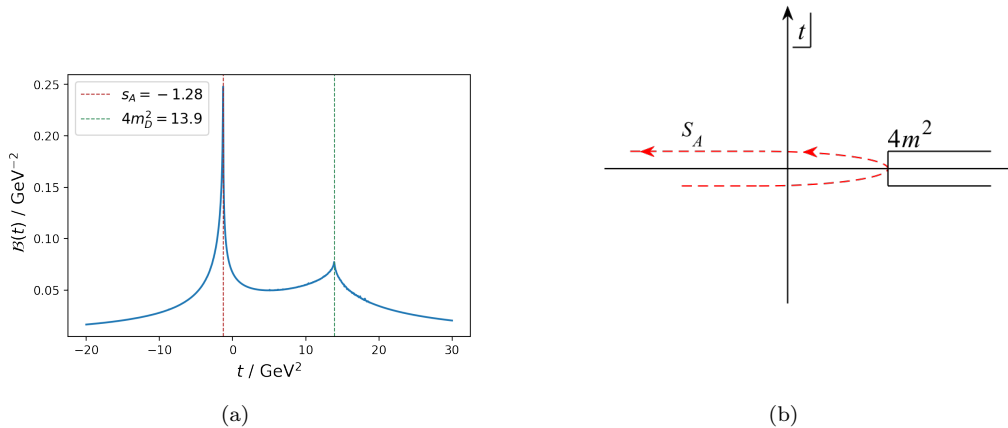


Figure 2: Left: triangle diagram contribution (the y axis label is arbitrary). Right: the trajectory of the anomalous threshold with respect to the variation of M^2 .

To proceed, one needs further to make the partial wave projection of \mathcal{M} and gets

$$T_{\mu_1\mu_2\mu_3\mu_4}^J(s) = \frac{1}{32\pi} \frac{1}{2q^2(s)} \int_{-4q^2(s)}^0 dt d_{\mu\mu'}^J \left(1 + \frac{t}{2q^2(s)} \right) \mathcal{M}_{\mu_1\mu_2\mu_3\mu_4}(t), \quad (7)$$

where the channel momentum square reads: $q^2(s) = (s - (M - M_J)^2)(s - (M + M_J)^2)/4s$ with M_J the mass of J/ψ , μ_i denotes the corresponding helicity configuration and $\mu = \mu_1 - \mu_2$, $\mu' = \mu_3 - \mu_4$. The key observation is that the integral interval in Eq. (7) will cover s_A if $\sqrt{s} > 6.96\text{GeV}$ (for D^+ loop, $\sqrt{s} > 6.94\text{GeV}$). In other words, the partial wave amplitude will be enhanced in the vicinity of $X(6900)$ peak by the anomalous threshold enhancement in the t channel, see Fig. 3 for illustration.

Based on the above observation it is suggested that the $X(6900)$ peak may at least partly be explained by the anomalous threshold generated by the triangle diagram as depicted in Fig. 1. Furthermore, to get the $L = 0$ (s wave) amplitudes, we need the relation between s wave and helicity amplitudes (see Refs. [11, 12] for more discussions):

$$T_{L=0}^{0,ij}(s) = \frac{1}{3} \left[2T_{++++}^{0,ij}(s) + 2T_{++--}^{0,ij}(s) - 2T_{++00}^{0,ij}(s) - 2T_{00++}^{0,ij}(s) + T_{0000}^{0,ij}(s) \right], \quad (8)$$

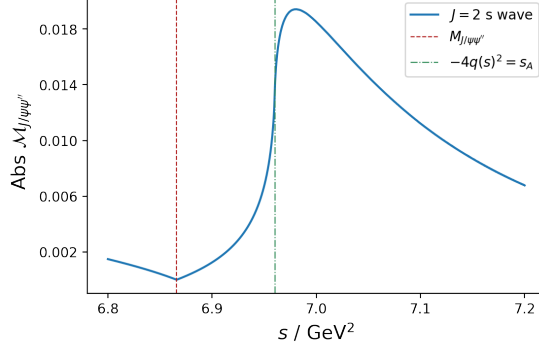


Figure 3: The enhancement of the $J/\psi\psi''$ scattering amplitude from the triangle diagram.

$$\begin{aligned}
T_{L=0}^{2,ij}(s) &= \frac{1}{15} [T_{++++}^{2,ij}(s) + T_{++--}^{2,ij}(s)] \\
&+ \frac{\sqrt{6}}{15} [T_{+++-}^{2,ij}(s) + T_{+-++}^{2,ij}(s) + T_{+-+-}^{2,ij}(s) + T_{-+++}^{2,ij}(s)] \\
&+ \frac{\sqrt{3}}{15} [T_{++++}^{2,ij}(s) + T_{+0++}^{2,ij}(s) + T_{++0+}^{2,ij}(s) + T_{0+++}^{2,ij}(s) \\
&+ T_{++-0}^{2,ij}(s) + T_{-0++}^{2,ij}(s) + T_{++0-}^{2,ij}(s) + T_{0-++}^{2,ij}(s)] \\
&+ \frac{1}{5} [T_{+00+}^{2,ij}(s) + T_{0+0+}^{2,ij}(s) + T_{+00-}^{2,ij}(s) + T_{0-+0}^{2,ij}(s) + T_{+0+0}^{2,ij}(s) \\
&+ T_{0+0+}^{2,ij}(s) + T_{0+0-}^{2,ij}(s) + T_{+0-0}^{2,ij}(s)] \\
&+ \frac{\sqrt{2}}{5} [T_{+-+0}^{2,ij}(s) + T_{+0+-}^{2,ij}(s) + T_{+-0+}^{2,ij}(s) + T_{0+--}^{2,ij}(s) \\
&+ T_{-++0}^{2,ij}(s) + T_{+0-+}^{2,ij}(s) + T_{-+0+}^{2,ij}(s) + T_{0+-+}^{2,ij}(s)] \\
&+ \frac{2}{15} [T_{++00}^{2,ij}(s) + T_{00++}^{2,ij}(s) + T_{0000}^{2,ij}(s)] + \frac{2\sqrt{6}}{15} [T_{+-00}^{2,ij}(s) + T_{00+-}^{2,ij}(s)] \\
&+ \frac{2}{5} [T_{+-+-}^{2,ij}(s) + T_{+--+}^{2,ij}(s)] + \frac{2\sqrt{3}}{15} [T_{+000}^{2,ij}(s) + T_{00+0}^{2,ij}(s) + T_{0+00}^{2,ij}(s) + T_{000+}^{2,ij}(s)] ,
\end{aligned} \tag{9}$$

where $i, j = 1, 2, 3$ denote the corresponding outgoing and incoming channels (corresponding to $J/\psi J/\psi$, $J/\psi\psi(3685)$ and $J/\psi\psi(3770)$, respectively). In practice, it is found that the anomalous enhancement gives a more prominent effect to the $J = 2$ amplitude than the $J = 0$ amplitude. The amplitude $T_{L=0}^{J,ij}$ is a K -matrix unitarized amplitude obtained from the tree level amplitudes generated from the following contact interaction lagrangian:

$$\begin{aligned}
\mathcal{L}_c &= c_1 V_\mu V_\alpha V^\mu V^\alpha + c_2 V_\mu V_\alpha V^\mu V'^\alpha + c_3 V_\mu V'_\alpha V^\mu V'^\alpha + c_4 V_\mu V'^\mu V_\alpha V'^\alpha + c_5 V_\mu V_\alpha V^\mu V''^\alpha \\
&+ c_6 V_\mu V'_\alpha V^\mu V''^\alpha + c_7 V_\mu V''^\mu V_\alpha V''^\alpha + c_8 V_\mu V'_\alpha V^\mu V''^\alpha + c_9 V_\mu V'^\mu V_\alpha V''^\alpha ,
\end{aligned} \tag{10}$$

The production amplitudes F_i^J are parameterized as,

$$F_i^J(s) = \sum_{k=1}^3 \alpha_k(s) T_L^{J,ki}(s) , \tag{11}$$

where $\alpha_k(s)$ are real polynomial functions in general and are set to be constants here, and further we set $\alpha_1(s)^2 = 1$. Further,

$$\frac{dEvents_i}{d\sqrt{s}} = N_i p_i(s) |F_i|^2 , \tag{12}$$

where $p_i(s)$ refers to the abs of three momentum for corresponding channel. According to partial wave convention, for $J = 0$ and $J = 2$ case, they have a total scale factor that [11, 12]

$$|F_i|^2 = |F_i^{J=0}|^2 + 5 |F_i^{J=2}|^2 . \tag{13}$$

The fit is overdone since there are many parameters. One solution is shown in Fig. 4, and the fit parameters are listed in Tab. 1 for illustration. During the fit many solutions are examined,

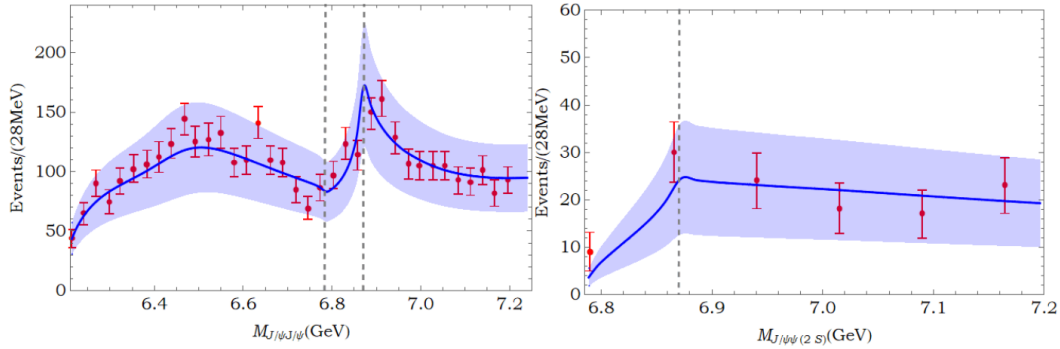


Figure 4: The fit results from table 1.

nevertheless it is found that the triangle diagram contributions are all small. It is not totally clear to us why it behaves like such but one possible reason could be that the peak position through anomalous threshold contribution, as shown in Fig. 3, is roughly 60 – 80MeV above the $X(6900)$ peak, and hence the fit does not like it. One possible way to rescue the problem may be to adopt another parameterization in which the background contributions are more flexible to be tuned, hence the interference between the background and the anomalous enhancement can lead to the shift of the peak position by a few tens of MeV. We leave this investigation for future studies.

Parameter	$\chi^2/d.o.f$	g'	N_1	N_2	α_2	α_3
Fit	0.93	-18.3 ± 1.6	23 ± 10	0.34 ± 0.23	-4.94 ± 0.02	3.97 ± 0.05
	c_5	c_6	c_7	c_8	c_9	
	11.34 ± 0.05	50.79 ± 0.05	-35.01 ± 0.19	-64.71 ± 0.07	1.529 ± 0.002	

Table 1: The fit parameters of Fig. 4. The c_i parameters are defined in Eq. (10). In this fit, we set c_1, \dots, c_4 to be negligible.

Acknowledgements

We would like to thank De-Liang Yao and Ling-Yun Dai for very helpful discussions. This work is supported in part by National Nature Science Foundations of China under Contract Number 12335002.

References

- [1] R. Aaij *et al.* (LHCb Collaboration), Sci.Bull. **65** (2020) 23, 1983.
- [2] CMS collaboration, CMS-PAS-BPH-21-003 (2022).
- [3] ATLAS collaboration, ATLAS-CONF-2022-040 (2022).
- [4] Y. Lu *et al.*, Phys. Rev. D**107** (2023) 094006.
- [5] Q. F. Cao *et al.*, Chin. Phys. C **45** (2021) 10, 103102.
- [6] D. Morgan, Nucl. Phys. A **543** (1992) 632.
- [7] O. Zhang, C. Meng and H. Q. Zheng, Phys. Lett. B **680** (2009) 453.
- [8] L. Y. Dai, M. Shi, G. Y. Tang and H. Q. Zheng, Phys. Rev. D **92** (2015) 014020.

- [9] Q. R. Gong, Z. H. Guo, C. Meng, G. Y. Tang, Y. F. Wang and H. Q. Zheng, Phys. Rev. D **94** (2016) 114019.
- [10] Q. F. Cao, H. R. Qi, Y. F. Wang and H. Q. Zheng, Phys. Rev. D **100** (2019) 054040.
- [11] Z. R. Liang, X. Y. Wu, D. L. Yao, Phys. Rev. D **104** (2021) 034034.
- [12] Q. Zhou, D. Guo, S. Q. Kuang, Q. H. Yang and L. Y. Dai, Phys. Rev. D **106** (2022) 11.
- [13] S. Mandelstam, Phys. Rev. Lett. **4** (1960) 84.
- [14] E. Braaten, H. W. Hammer, Phys. Rep. **428** (2006) 259.
- [15] H. W. Hammer, C. Ji and D. R. Phillips, J. Phys. G **44** (2017) 103002.
- [16] M. Tanabashi *et al.* (Particle Data Group), Phys. Rev. D **98** (2018) 030001.
- [17] S. Coito and F. Giacosa, Nucl. Phys. A **981** (2019) 38.